General and Comparative Endocrinology 360 (2025) 114641

Contents lists available at ScienceDirect

General and Comparative Endocrinology

journal homepage: www.elsevier.com/locate/ygcen

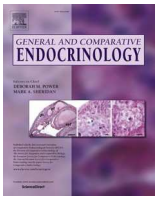

Spatial and quantitative gene expression analysis of SREB receptors in the gonads of green-spotted pufferfish (*Dichotomyctere nigroviridis*)

Timothy S. Breton [a,*], Maria Eduarda Oliveira [a], Truly Chillemi [a], William Harriman [a], Joanna Korasadowicz [a], Eme Saverese [a], Emma Bourget [a], Casey A. Murray [b], Christopher J. Martyniuk [c], Matthew A. DiMaggio [b]

[a] *Biology Department, University of Maine at Farmington, Farmington, ME 04938, USA*
[b] *Tropical Aquaculture Laboratory, Program in Fisheries and Aquatic Sciences, School of Forest, Fisheries, and Geomatics Sciences, Institute of Food and Agricultural Sciences, University of Florida, Ruskin, FL 33570, USA*
[c] *Center for Environmental and Human Toxicology, Department of Physiological Sciences, College of Veterinary Medicine, University of Florida, Gainesville, FL 32611, USA*

ARTICLE INFO

Keywords:
GPR27
GPR85
GPR173
SREB
Reproduction
Oocyte
Spermatogonia

ABSTRACT

Super-conserved Receptors Expressed in Brain (SREB) are a highly conserved family of orphan G protein-coupled receptors that consist of three members in most vertebrates: SREB1 (GPR27), SREB2 (GPR85), and SREB3 (GPR173). Each receptor is associated with diverse physiological processes and expressed in both ovaries and testes, but reproductive functions are only beginning to be understood. In addition, some fishes gained a novel fourth gene, SREB3B, which may have unique functions. The purpose of this study was to conduct a spatial and quantitative analysis of SREBs in the gonads of pufferfish (*Dichotomyctere nigroviridis*), which expresses all four genes. Multiplex RNAscope and absolute qPCR were used to assess gene expression patterns in both ovaries and testes. Expression was detected in early ovaries and dominated by *sreb1* (approximately 2500 copies/ng RNA vs. 300 or less for others), with notable expression of all receptors in primary oocytes, granulosa cells, and small numbers of extra-follicular cells. Within primary oocytes, *sreb1* and *sreb3b* exhibited diffuse patterns that may indicate early functions, while *sreb2* and *sreb3a* were granular and may reflect stored mRNA. Early testicular development was dominated by *sreb1* and *sreb2* (~5000 copies/ng RNA) in spermatogonia. These patterns were somewhat reduced in late testes (~1000–2600 copies/ng RNA), but *sreb3b* exhibited a novel spatial pattern (~380 copies/ng RNA) within spermatogenic cysts. These results highlight diverse roles for the SREB family, and *sreb3b* is hypothesized to have unique roles in fish reproduction.

1. Introduction

Super-conserved receptors expressed in brain (SREB) are a family of Class A rhodopsin-like G protein-coupled receptors (GPCRs) that are among the most highly conserved receptor genes across vertebrate evolution (O'Dowd et al., 1998; Hellebrand et al., 2000; Matsumoto et al., 2000). Most vertebrates exhibit three members (SREB1, SREB2, and SREB3), but their functions remain largely elusive due to a lack of confirmed ligands, and the group is still identified as orphan receptors (GPR27, GPR85, and GPR173, respectively) (Stäubert et al., 2022). While all three exhibit elevated expression in neurons of the mammalian central nervous system, they are also expressed in many other organs and cell types, and each receptor is associated with a variety of physiological processes (Matsumoto et al., 2000, 2005).

SREB1 was examined as a novel GPCR regulator of insulin secretion in pancreatic beta cells, where it reduced insulin mRNA and had minor effects on glucose tolerance in mice (Regard et al., 2007; Ku et al., 2012; Chopra et al., 2020). In contrast, SREB2 has mostly been studied in the brain and plays roles in neurogenesis and memory (Chen et al., 2012). Brain size is affected in mice when SREB2 expression is perturbed, and the gene has been identified in humans as a risk factor for schizophrenia and autism spectrum disorder (Matsumoto et al., 2008; Fujita-Jimbo et al., 2015). The third family member, SREB3, has received the most recent research attention due to the identification of several unconfirmed potential ligands, including: 1) a cleavage product of a mitochondrial protein (phoenixin), 2) a metabolite of gonadotropin-

* Corresponding author.
E-mail address: timothy.breton@maine.edu (T.S. Breton).

https://doi.org/10.1016/j.ygcen.2024.114641
Received 19 August 2024; Received in revised form 21 October 2024; Accepted 9 November 2024

releasing hormone (GnRH(1–5)), and 3) a well-studied neuropeptide (cholecystokinin) (He et al., 2023; Larco et al., 2013; Mcilwraith and Belsham, 2018; Yosten et al., 2013). Collectively, these studies elucidate the roles of SREB3 in neuronal cells, including the mediation of inhibitory signals, cell migration, appetite regulation, and hypothalamic control of reproduction (He et al., 2023; Larco et al., 2018; Mcilwraith et al., 2022).

SREBs also play reproductive roles in gonads, as all members are expressed in ovaries and testes (Matsumoto et al., 2000). In the human ovary, SREB3 is expressed in granulosa cells and promotes growth and estradiol production during the follicular phase (Nguyen et al., 2019). Female reproductive tissues in some mammals exhibit SREB3 changes during polycystic ovary syndrome and cystic endometrial hyperplasia, respectively (Kalamon et al., 2020; Rybska et al., 2022, 2023). Ovarian roles may be highly conserved across vertebrates, as SREB3 was also detected in zebrafish (*Danio rerio*) granulosa cells and oocytes, and the protein promotes follicle growth and maturation (Rajeswari and Unniappan, 2020). Additionally, SREB3 is expressed in the zebrafish testis, and the entire SREB family in most fishes actually exhibits higher gene expression levels in testes compared to the ovaries (Rajeswari and Unniappan, 2020; Breton et al., 2021). However, the testicular roles for any SREB are poorly understood, and no studies to date have focused on SREB1 or SREB2 in any reproductive context. Perhaps the most significant knowledge gap is that these two genes have not yet been characterized spatially outside of the brain in any vertebrate.

Fish represent an intriguing vertebrate clade to study the SREB family. Fish are unique among vertebrates in that many species exhibit a novel fourth family member, SREB3B, which resulted from a gene duplication event of SREB3 following the teleost whole genome duplication (Breton et al., 2021). As a result, less derived fishes such as zebrafish lack SREB3B, while more derived species such as salmonids and percomorphs exhibit the additional gene. While SREB3B remains largely unstudied, there is some evidence to support: 1) divergent functions from SREB3A (the fish ortholog to mammalian SREB3), and 2) reproductive roles for the receptor. For instance, spotted scat (*Scatophagus argus*) hypothalamic cells exhibited different *sreb3a* and *sreb3b* gene expression changes when exposed to estradiol (Jiang et al., 2022). In addition, upstream genomic regions of *sreb3b*, but not *sreb3a*, exhibited highly conserved transcription factor binding sites related to ovarian growth and germ cell pluripotency (Breton et al., 2023). Overall though, more research is needed to better understand the novel receptor, its potential reproductive roles, and how it may be unique in spatial location from other gonadal SREBs.

The purpose of the present study was to conduct a detailed spatial and quantitative characterization of the entire SREB family in fish gonads, to better understand their expression patterns across different cell types and potential roles in reproduction. Based on evidence from past studies in other vertebrate systems, we hypothesize that most *sreb* genes exhibit similar expression patterns in both oocytes and follicle cells in ovaries, and in developing spermatogenic cells in testes. We also hypothesize that the novel fish-specific *sreb3b* will exhibit divergent spatial patterns from *sreb3a* in some gonadal cell types. To evaluate these hypotheses, green-spotted pufferfish (*Dichotomyctere nigroviridis*) was used, which is a highly derived species that exhibits all four genes, unlike zebrafish and some other fishes (Breton et al., 2021). In addition, pufferfish exhibit unique characteristics in their genome assembly that warrant investigation, including unverified annotations for *sreb1* and *sreb3a* that label them as both pseudogenes and protein-coding genes (Ensembl genome browser 112, TETRAODON 8.0). To address this, we used standard PCR to verify near full-length transcription of each *sreb* gene in pufferfish. Then, multiplex fluorescence RNAscope and absolute quantitative PCR (qPCR) were used to map expression patterns of all four genes across gonadal development in both ovaries and testes.

2. Material and methods

2.1. Pufferfish care and sampling

Wild-caught green-spotted pufferfish from Thailand were imported through a local wholesaler (Segrest Farms, LLC) in October 2023, and maintained in a 215 L tank supplied with flow-through degassed and filtered freshwater at the University of Florida (UF) Tropical Aquaculture Laboratory (Ruskin, FL, USA). All fish were maintained and sampled in accordance with guidelines from the UF Institutional Animal Care and Use Committee (IACUC #202300000749) regarding ethical vertebrate animal use. Approval was also provided by the University of Maine at Farmington (UMF) Grant Coordination Committee, and all experiments were conducted in compliance with ARRIVE guidelines.

To identify a variety of ovarian and testicular stages and promote gonadal development, fish were acclimated to saltwater (30 g/L salinity) over 14 days and periodically sampled across four months (October 2023 – February 2024). All fish were euthanized with 500 mg/L neutral-buffered tricaine methanesulfonate (MS-222; Syndel, Ferndale, WA, USA), weighed, measured (total length, mm) and gonads were removed. Gonadal fragments from each fish were: 1) placed in a cryomold and submerged in Optimal Cutting Temperature (OCT) compound for spatial analyses in RNAscope, and 2) preserved in RNALater (Ambion, Inc., Austin, TX, USA) for PCR-based analyses. All gonadal samples were immediately frozen on dry ice, preserved at −80 °C, and shipped frozen to UMF laboratories for gene expression analyses.

2.2. RNA extractions and confirmation of sreb transcription

RNA extractions for PCR-based analyses were performed on primary and early secondary stage ovaries (n = 8, mean total length = 62.9 ± 1.6 mm, mean weight = 7.2 ± 0.6 g), vitellogenic ovaries (n = 5, 60.4 ± 1.4 mm, 7.1 ± 0.4 g), early developing testes (n = 7, 67 ± 1.7 mm, 9.9 ± 1.7 g), and mid-late testes (n = 5, 65.8 ± 3.8 mm, 9.6 ± 1.7 g). All samples were homogenized in Tri Reagent (Sigma-Aldrich, St. Louis, MO, USA) and used in standard phenol/chloroform procedures. Most vitellogenic ovaries required an additional incubation using a polyvinylpyrolidone (PVP) solution (2 % PVP, 1.4 M NaCl) and a lithium chloride precipitation to remove polysaccharide contamination (Picha et al., 2008). RNA quantity and quality were checked using a NanoDrop 2000 spectrophotometer (Thermo Fisher Scientific, Waltham, MA, USA) and 1 % agarose gel electrophoresis. All samples exhibited high quality (absorbance ratios 260/280 and 260/230 of ~ 2.0 and > 2.0, respectively) with intact rRNA bands. Total RNA (1.67–2.50 μg) was treated with ezDNase and a 5 min incubation step at 37 °C to remove genomic DNA contamination, followed by cDNA synthesis using Superscript IV VILO (Invitrogen, Carlsbad, CA, USA).

To confirm that each *sreb* gene was likely fully transcribed for later analyses, standard PCR and 2 % agarose gel electrophoresis were performed on selected cDNA samples (n = 2/stage). Samples were used in PCR with the Promega GoTaq Flexi PCR kit (Promega, Madison, WI, USA) following standard protocols (Breton et al., 2019). Standard PCR primers (two sets per gene) were designed to: 1) include most of the protein-coding sequence intended for use in RNAscope probes (see Section 2.3), and 2) flank regions previously validated in each gene using qPCR primers (Breton et al., 2021). All primer sets were designed for a 60 °C annealing temperature and are provided in Supplementary Table 1. PCR products were used in agarose gel electrophoresis following standard protocols and imaged to observe expected banding patterns. Negative controls (no reverse transcriptase and no template) exhibited no amplification.

2.3. Multiplex RNAscope

Selected primary and early secondary stage ovaries (total n = 7), vitellogenic ovaries (n = 3), early developing testes (n = 3), and mid-late

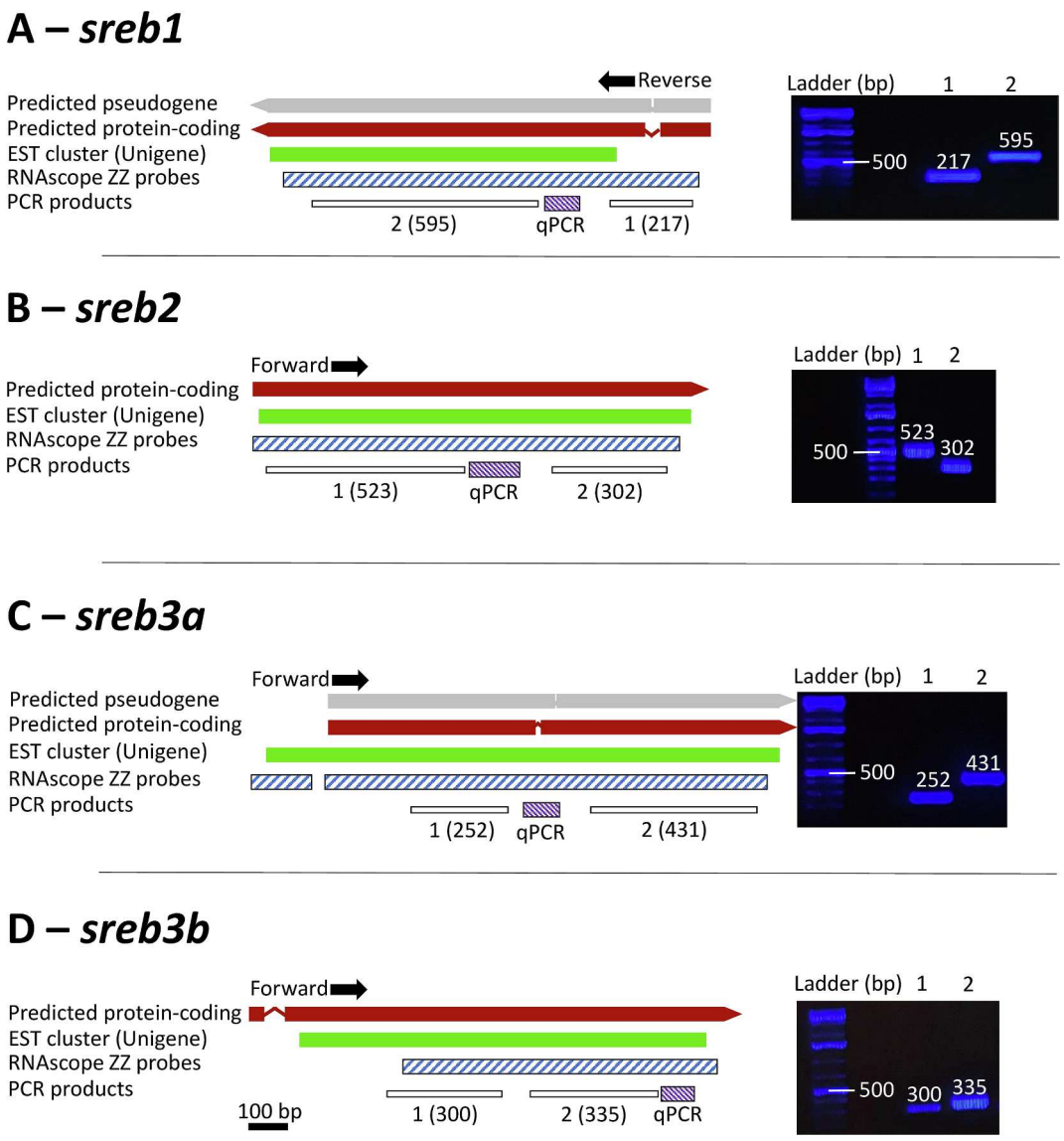

Fig. 1. Ensembl genome browser 112 features (left) and representative agarose gel electrophoresis (right) of PCR products from cDNAs for pufferfish *sreb1* (A), *sreb2* (B), *sreb3a* (C), and *sreb3b* (D). Predicted pseudogenes, protein-coding regions, and EST cluster transcripts identified in Unigene are labeled in gray, red, and green, respectively. Transcript regions used for RNAscope probe synthesis and qPCR are labeled in blue and purple stripes, respectively. Additional two PCR-amplified regions (1, 2) used to confirm transcription of each gene at RNAscope probe sites are shown in white bars with intended product sizes (base pairs, bp). Representative gel images for all genes reflect similar results across all four gonadal stages. Black bar refers to 100 bp.

testes (n = 5) were used in multiplex RNAscope to identify mRNA spatial expression patterns within each organ and developmental stage. Briefly, fresh frozen gonadal fragments in OCT were sectioned at 10 μm in a −20 °C equilibrated cryostat (Leica CM1850), mounted onto SuperFrost Plus slides (VWR International, LLC, Radnor, PA, USA), dried for approximately 1 hr at −20 °C, and stored in a slide box wrapped in aluminum foil at −80 °C for up to three days prior to use.

Pufferfish-specific double-Z probes for multiplex RNAscope were designed by Advanced Cell Diagnostics (ACD) (Hayward, CA, USA). Previously identified pufferfish *sreb1*, *sreb2*, *sreb3a*, and *sreb3b* sequences were used (Breton et al., 2021) to identify protein coding regions in ORFfinder (see Supplementary Data) and used to generate 12ZZ (designed for channel 1), 20ZZ (2), 12ZZ (3), and 10ZZ (4) probe sets targeting nucleotide positions 32–1101, 2–1107, 2–1341, and 27–814, respectively. In addition, probe sets for positive control genes *actb1* (GenBank Accession No. CR695870.2), *eef1a* (Ensembl Tetraodon gene ENSTNIT00000017382.1), *zp3f* (Ensembl gene ENSTNIT00000010945.1), and *dmrt1* (Ensembl gene ENSTNIT00000018941.1) were used to generate 11ZZ (1), 17ZZ (2), 20ZZ (3), and 15ZZ (4) probe sets targeting nucleotide positions 2–1845, 45–1036, 2–936, and 85–842, respectively. A 4-plex negative control probe set for bacterial gene dapB was also used (ACD Cat. No. 321831). Target probe sequences are proprietary but can be purchased from ACD (Wang et al., 2012).

Due to imaging limitations with fluorophores, all target probes were used in 3-plex combinations. Briefly, positive control genes were sorted into two multiplexes to alternate between an ovary-specific (*zp3f*) or testis-specific (*dmrt1*) gene. Control Multiplex 1 consisted of *actb1*, *eef1a*, and *zp3f*, while Control Multiplex 2 consisted of *actb1*, *eef1a*, and *dmrt1*. Both control multiplexes were used in ovary and testis sections to validate expected expression patterns. Control Multiplex 3 consisted of the ACD negative control dapB probe mix. Probes for *sreb* genes were also used in multiplex combinations. Multiplex 1 consisted of *sreb1*, *sreb3a*, and *sreb3b*, which was designed to investigate potential co-localization between the two *sreb3* paralogs in fish (Breton et al., 2021). Multiplex 2 consisted of *sreb1*, *sreb2*, and *sreb3b*, which was

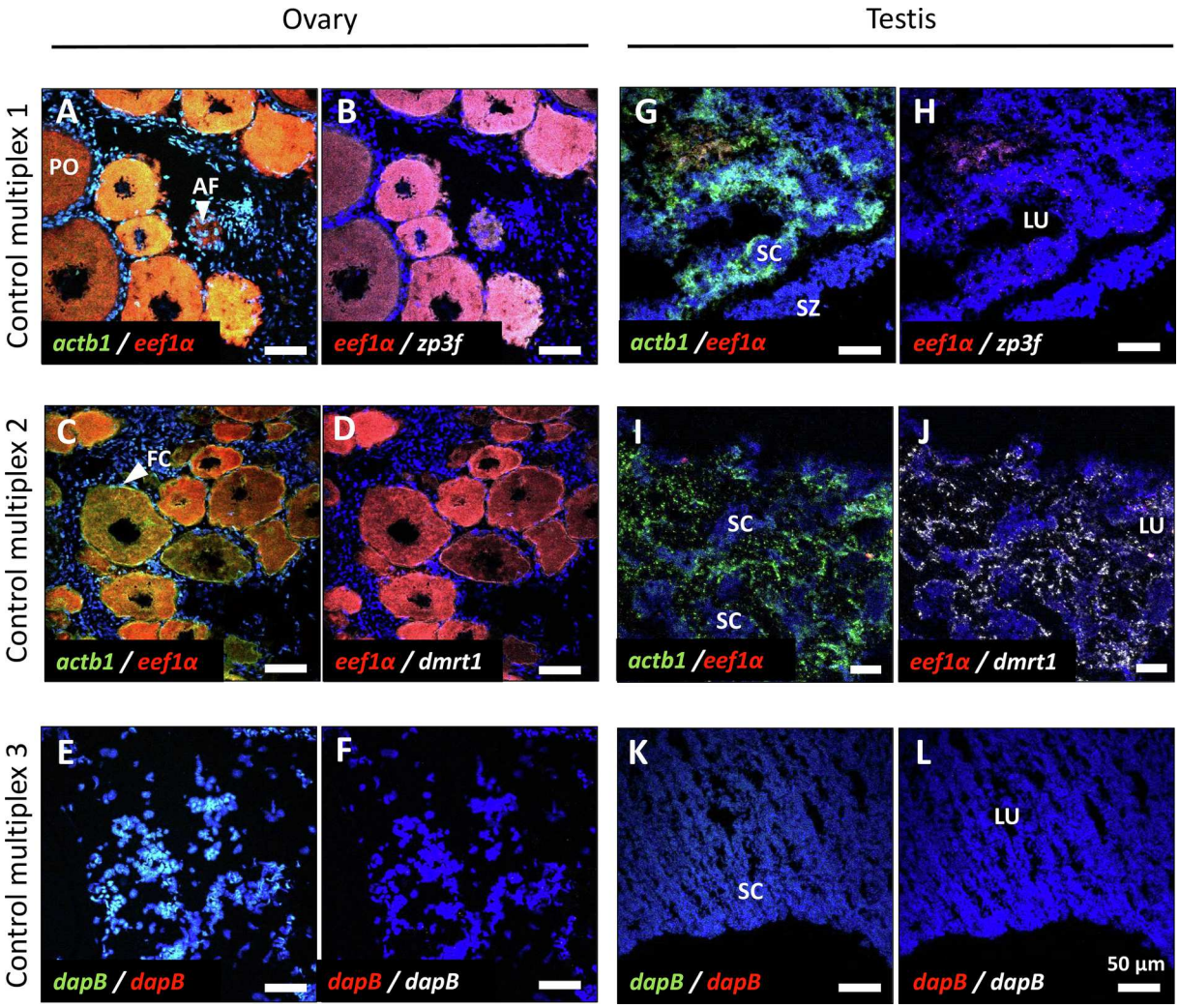

Fig. 2. Multiplex RNAscope pufferfish ovary positive (A-D), ovary negative (E, F), testis positive (G-J), and testis negative (K, L) controls. Control Multiplexes 1, 2, and 3 refer to 3-plex probe combinations of: 1) *actb1*, *eef1a*, and *zp3f*, 2) *actb1*, *eef1a*, and *dmrt1*, or 3) bacterial gene dapB, respectively. Scale bars refer to 50 µm. Cell nuclei are stained blue using DAPI, and *actb1* and *eef1a* are labeled green and red, respectively, while *zp3f* and *dmrt1* are labeled white. AF = atretic follicle; LU = lumen of testicular lobule; PO = primary oocyte; SC = spermatocytes; SZ = spermatozoa.

designed to investigate potential similarity in spatial patterns between the highly conserved latter two genes (Breton et al., 2021). Multiplexes 1 and 2 were used in all gonad samples previously described, except for primary and early secondary growth ovaries (n = 3). Since neither multiplex could evaluate co-localization within oocytes between *sreb2* and *sreb3a* simultaneously, a third multiplex of only these two genes (Multiplex 3) was used in additional primary growth ovary samples (n = 4).

Multiplex RNAscope was conducted following recommended protocols in the RNAscope Multiplex Fluorescent Kit v2 (ACD Cat. No. 323100) and 4-Plex Ancillary Kit (ACD Cat. No. 323120). Briefly, slides with gonadal sections were incubated at 4 °C in 10 % neutral-buffered formalin for 1 hr, then rinsed twice with 1X phosphate buffered saline, dehydrated in an ethanol series, and treated with hydrogen peroxide for 10 min and Protease IV for 30 min at room temperature following manufacturer's instructions. Slides were then incubated with prepared probe multiplexes in the HybEZ II oven (ACD) for 2 hr at 40 °C. Positive and negative control multiplex slides were used in every RNAscope procedure and run alongside Multiplexes 1, 2, or 3. Each positive control or *sreb* probe was used in at least two multiplexes, except for the expected ovary or testis-specific markers *zp3f* and *dmrt1*, respectively. Following recommended steps, Amps 1, 2, and 3 were then hybridized to the slides, and HRP-C1, HRP-C2, and either HRP-C3 or HRP-C4 (depending on multiplex) signals were developed. To visualize each channel, Opal fluorophores 520 (channel 1), 570 (channel 2), and 620 (channel 3 or 4) (Akoya Biosciences, Marlborough, MA, USA) were used at a recommended concentration of 1:1500 by ACD. Opal fluorophores were prepared as recommended by Akoya Biosciences and the 4-Plex Ancillary Kit. After signal development, DAPI was added to each slide to stain cell nuclei, incubated for 30 s, removed, and Prolong Gold antifade mounting medium (Fisher Scientific, Wilmington, DE, USA) was added. Coverslips were then placed, and slides were dried overnight in the dark before storage at 4 °C.

2.4. Confocal microscopy and co-localization analysis

All slides were first examined for fluorescence within 24–48 hrs of the completed RNAscope procedure using a FluoView FV1000 confocal microscope (Olympus Life Science, Waltham, MA, USA) with 10X, 20X, and 40X UplanSApo or 60X PlanSApo (oil immersion) objective lenses. Images were acquired using simultaneous capture of up to three fluorophores with standard settings, including low Gain, low Offset, and HV levels generally between 600 and 750 (Olympus FluoView-1000 User's Guide, V.M. Bloedel Hearing Research Center, Digital Microscopy Center, University of Washington). Opal 520, 570, and 620 fluorescence were imaged using recommended filter settings FITC, Cy3, and Cy5.5 (4-

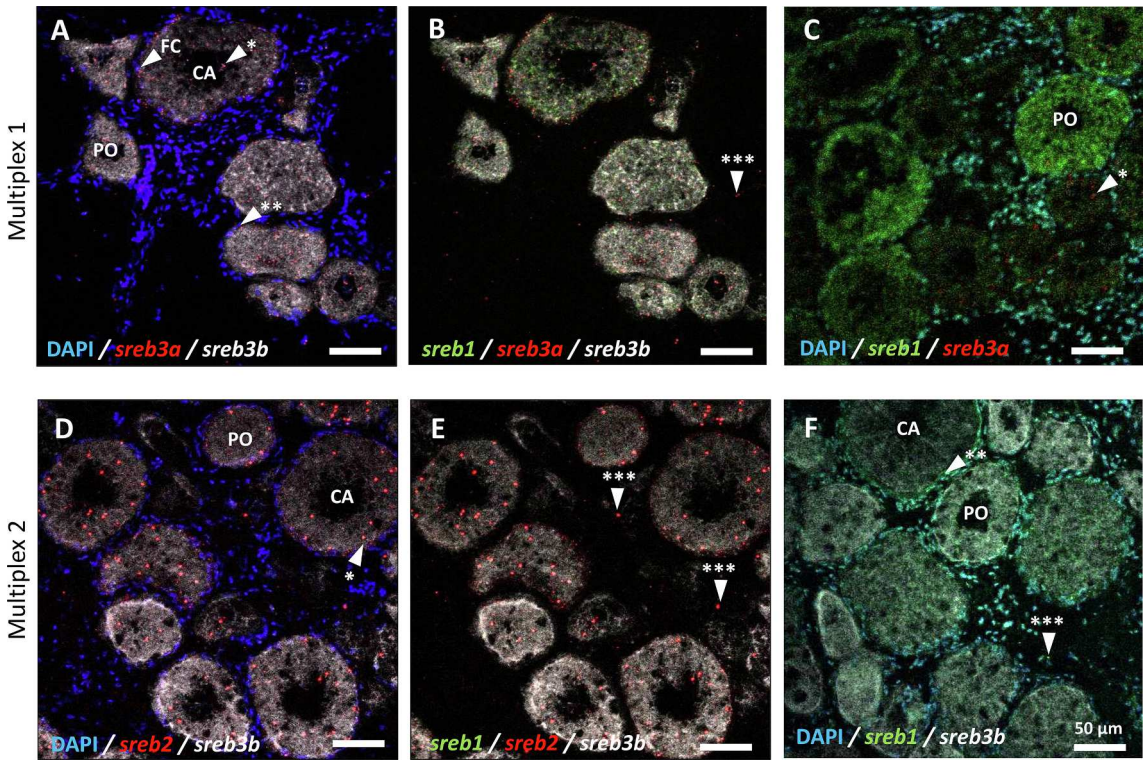

Fig. 3. Multiplex RNAscope of primary and early secondary growth pufferfish ovaries using Multiplex 1 (*sreb1*, *sreb3a*, and *sreb3b*; A-C) or Multiplex 2 (*sreb*1, *sreb2*, *sreb3b*; D-F). Scale bars refer to 50 µm. Cell nuclei are stained blue using DAPI, and *sreb1* and *sreb3b* are labeled green and white, respectively, while *sreb2* and *sreb3a* are labeled red. CA = cortical alveoli stage or early secondary oocyte; FC = follicle cells; PO = primary oocyte. * indicates dotted *sreb* pattern within ooplasm. ** indicates follicle cell expression with overlapping DAPI. *** indicates stromal cell expression not associated with an ovarian follicle.

Plex Ancillary Kit).

To assess potential *sreb* co-localization within primary growth oocytes, a correlation-based method was used in the Coloc2 package within Fiji/ImageJ (Schindelin et al., 2012, Mascalchi and Cordelières, 2019). Single channel images of every ovary sample in each multiplex were taken using the 40X UplanSApo lens. Each sample was imaged in three random locations within the ovary where at least three primary follicles were visible. Images were then imported into Fiji, converted to 16-bit, and the freehand tool was used to identify regions of interest (ROIs) consisting of three randomly chosen individual primary oocytes in each image. One vitellogenic ovary sample mostly lacked primary growth follicles and was removed from some comparisons. Pairwise single channel images with oocyte ROIs were then compared using standard parameters in Coloc2 to calculate Pearson's R value, which provides a measure of correlation between two signals. Since this method was expected to exhibit high variability, the procedure was validated by including Positive Control Multiplex 1 genes in the pairwise comparisons. These genes were expected to exhibit greater positive values than *sreb* genes due to abundant oocyte expression throughout the ooplasm. In addition, the *sreb1* vs. *sreb3b* comparison was performed twice because these genes were run simultaneously in both Multiplex 1 and 2, and similar mean values were expected. The pairwise comparisons in Coloc2 consisted of the following ovary sample sizes and individual oocyte ROIs: 1) *actb1* vs. *eef1a* (fish n = 5 and oocyte n = 45), 2) *eef1a* vs. *zp3f* (n = 5 and 45), 3) *actb1* vs. *zp3f* (n = 5 and 45), 4) *sreb1* vs. *sreb3a* (n = 5 and 45), 5) *sreb1* vs. *sreb3b* (Multiplex 1, n = 5 and 45), 6) *sreb1* vs. *sreb3b* (Multiplex 2, n = 6 and 51), 7) *sreb3a* vs. *sreb3b* (n = 5 and 45), and 8) *sreb2* vs. *sreb3a* (n = 4 and 36). Pearson's R values were square root transformed to meet normality and equal variance assumptions and used in one-way ANOVA in SYSTAT12 (Systat Software Inc., San Jose, CA, USA). Tukey's post hoc tests were used to identify significant differences in R values among pairwise comparisons ($p < 0.05$).

2.5. Absolute quantitative PCR

To directly compare expression levels across *sreb* genes, absolute quantitative PCR (qPCR) was performed using all RNA-extracted gonadal samples (see section 2.2). While a prior study in pufferfish used relative quantitative PCR to assess gonadal *sreb* patterns (Breton et al., 2021), this approach was limited and could not statistically compare gene levels across different transcripts. As such, absolute qPCR was used in this study to quantify transcript copy numbers and characterize if some receptor types are predominant or only weakly expressed in the gonads. Previously designed qPCR primers (Breton et al. 2021, Supplementary Table 1) were used in a StepOne Plus Real Time PCR System with FAST SYBR™ Green Master Mix (Applied Biosystems, Waltham, MA, USA). Synthetic oligonucleotides for each pufferfish *sreb* gene were purchased as gBlocks™ gene fragments (see Supplementary Data) from Integrated DNA Technologies (IDT, Coralville, IA, USA), resuspended following IDT protocols, and diluted to 10^6 copies/µl for use in standard curves. Standards were serially diluted 1/10 following established protocols (Conte et al., 2018), and quantitative results for all assays were demonstrated down to 100 copies/µl, after which cycle threshold (Ct) values exceeded 32–34. Pooled cDNA samples across all stages were also used in relative standard curves at the same PCR conditions to demonstrate similar amplification. All assays were conducted in 10 µl total volumes with 1.33 µl template, 0.05–0.2 µM primers (depending on assay), 50 ng/µl bovine serum albumin (BSA) to minimize potential inhibitor effects (Schriewer et al., 2011), and standard cycling conditions (95 °C for 10 min, 40 cycles of 95 °C for 15 s and 60 °C for 1 min). All gBlock curves and relative sample standard curves were run in triplicate, consisted of at least four points, and exhibited approximately 90–110 % PCR efficiency. Following assay validation, an additional gBlock standard curve was run with all cDNA samples (diluted 1/10) in the same 96-well plate for quantification. All samples were assayed in duplicate and exhibited single peak amplification in

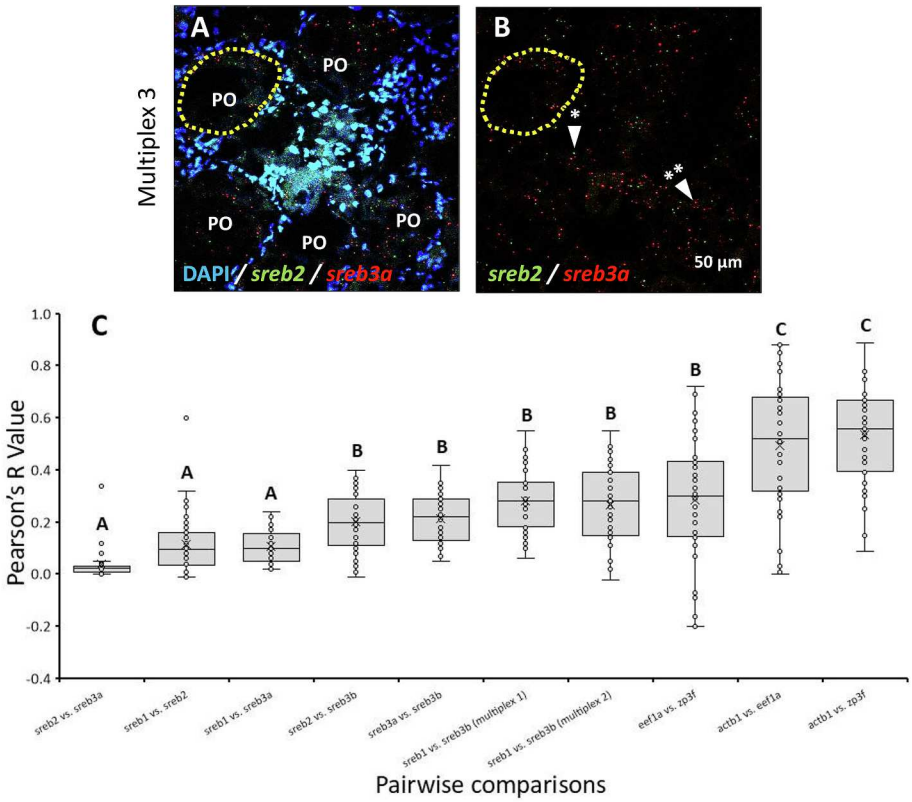

Fig. 4. RNAscope Multiplex 3 (*sreb*2 and *sreb3a*) (A, B) and co-localization analysis across all gene pairwise comparisons in primary and early secondary growth pufferfish ovaries (C). Cell nuclei are stained blue using DAPI, and *sreb2* and *sreb3a* are labeled green and red, respectively. Yellow dotted areas encircle oocyte regions of interest (ROIs) used in co-localization analysis in Fiji. Scale bar refers to 50 µm. Significant differences in Pearson's R value across gene pairwise comparisons are indicated by different letters ($p < 0.05$). Pairwise comparisons are sorted based on ascending median Pearson's R values. PO = primary oocyte. * and ** indicate *sreb2* and *sreb3a* dotted patterns in ooplasm, respectively.

dissociation curve analysis. Standard qPCR negative controls (no template and no reverse transcriptase) exhibited no contamination. Additional pooled cDNA samples (n = 2/assay) were also spiked with gBlock standards using two different known concentrations and quantified, which resulted in 91.8 % mean recovery of expected values across all assays.

Copy number/µl results were normalized to input RNA quantity, and each assay was contained in a single 96-well plate (Campbell et al., 2006). Data were log-transformed to meet assumptions of normality and used in one-way ANOVAs in SYSTAT12. Tukey's post hoc tests were used to identify significant differences across genes within each gonadal stage ($p < 0.05$).

3. Results

3.1. Confirmation of sreb transcription

Each pufferfish *sreb* gene exhibited evidence of transcription in all gonadal stages (Fig. 1). Primers that flanked previously validated qPCR transcripts exhibited expected PCR banding patterns, and no differences were detected between genes predicted as pseudogenes (*sreb1* and *sreb3a*, Fig. 1A, C) and those identified only as protein-coding genes (*sreb2* and *sreb3b*, Fig. 1B, D). Evidence of transcription was also evident in the 5′ end of *sreb1*, which did not share similarity to expressed sequence tags (ESTs) from other species in Unigene (Fig. 1A). Overall, all *sreb* protein-coding regions selected for RNAscope probes were identified as transcriptionally active.

3.2. RNAscope positive and negative controls

Ovary positive control genes *actb1*, *eef1a*, and *zp3f* were all abundantly expressed in primary growth stage oocytes (Fig. 2A, B). When the ovary-specific gene *zp3f* was replaced with testis marker *dmrt1* in Control Multiplex 2, abundant expression of both *actb1* and *eef1a* were retained in oocytes while *dmrt1* signals were low (Fig. 2C, D). Ovary negative controls for the dapB bacterial gene exhibited no apparent signals in any channel (Fig. 2E, F).

Testis positive control genes *actb1* and *eef1a* exhibited abundant expression, especially in areas around the periphery of testicular lobules (Fig. 2G). In contrast, the third gene and ovary-specific marker (*zp3f*) in Control Multiplex 1 exhibited no notable expression in testis (Fig. 2H). When *zp3f* was replaced with testis marker *dmrt1*, abundant expression was detected throughout the tissues along with retention of the *actb1* and *eef1a* signals (Fig. 2I, J). Testis negative controls with dapB exhibited no signals (Fig. 2K, L).

3.3. Ovary spatial sreb patterns and co-localization within primary oocytes

Expression patterns within oocytes differed among *sreb* genes (Fig. 3). For instance, *sreb3b* was present as a diffuse signal throughout the ooplasm of primary (PO) and early secondary growth (CA, cortical alveoli) oocytes, while *sreb3a* exhibited a more dotted pattern in discrete locations (indicated by * in Fig. 3A). Signals for *sreb1* were more similar to *sreb3b* and diffuse (Fig. 3B, C). The *sreb2* signals most closely matched *sreb3a*, with a clear dotted patterning in the ooplasm (see Multiplex 2 in Fig. 3D, E). The *sreb1* and *sreb3b* patterns were also diffuse in the ooplasm in this multiplex (Fig. 3F). Overall weak expression was also

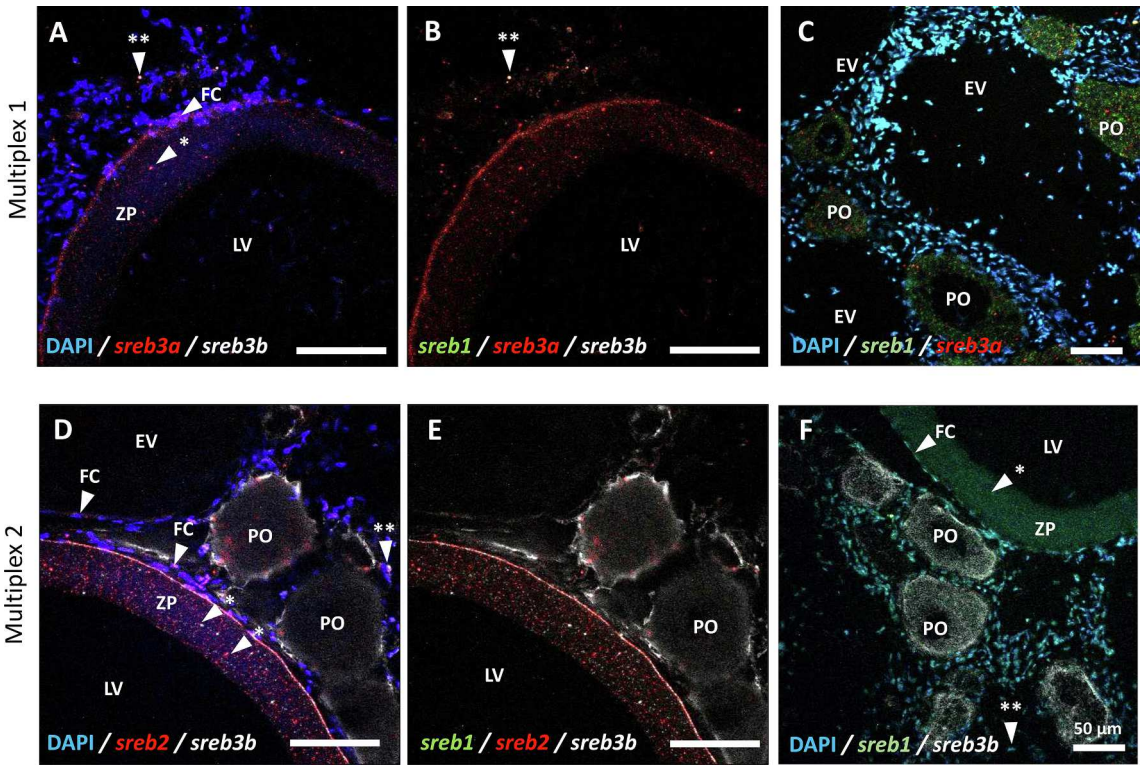

Fig. 5. Multiplex RNAscope of vitellogenic stage pufferfish ovaries using Multiplex 1 (*sreb1*, *sreb3a*, and *sreb3b*; A-C) or Multiplex 2 (*sreb*1, *sreb2*, *sreb3b*; D-F). Scale bars refer to 50 µm. Cell nuclei are stained blue using DAPI, and *sreb1* and *sreb3b* are labeled green and white, respectively, while *sreb2* and *sreb3a* are labeled red. EV = early vitellogenic oocyte; FC = follicle cells; LV = late vitellogenic oocyte; PO = primary oocyte; ZP = zona pellucida. * and ** indicate *sreb* patterns within the ZP and extra-follicular cells, respectively.

detected in granulosa cells surrounding oocytes (indicated by ** in follicle cell (FC) layers) and in several locations in stromal cells not associated with ovarian follicles (*** in Fig. 3B, E, F).

The dotted patterns for both *sreb2* and *sreb3a* in early stage oocytes were confirmed in a third multiplex using early growth stage (PO) oocytes (see * and ** in Fig. 4A, B). However, these signals exhibited no similarity to each other and did not co-localize to the same locations in ooplasm, as Pearson's R values were largely near zero (Fig. 4C). In addition, no significant oocyte co-localizations were detected in any gene pairwise comparisons among *sreb1*, *sreb2*, or *sreb3a*. However, *sreb3b* exhibited moderate but significant co-localization with all other *sreb* genes, and this was at least partially validated across two multiplexes (see *sreb1* vs. *sreb3b* comparisons, Fig. 4C). As expected, most Control Multiplex 1 genes exhibited the greatest significant correlations to each other, except for *eef1a* vs. *zp3f*, which was the most variable of all pairwise comparisons but did exhibit a greater median value than any of the *sreb* genes (Fig. 4C).

Vitellogenic oocytes at either early (EV) or late growth (LV) largely did not exhibit *sreb* signals within the ooplasm, except within the zona pellucida (ZP) and at its outer edge (* in Fig. 5). This was similar to patterns observed in control genes (data not shown). All *sreb* genes exhibited these patterns and were largely similar to each other. Granulosa cells in the follicle layers immediately peripheral to the zona pellucida also exhibited expression at these stages, as well as in extra-follicular cells (** in Fig. 5A,B, D, F).

3.4. Testis spatial sreb patterns

The early developing testis was characterized overall by widespread *sreb1* and *sreb2* expression but more moderate levels for *sreb3a* and *sreb3b* (ET in Fig. 6). These same patterns were largely spread across the entire organ, with the only differing characteristic among *sreb* genes being particularly abundant *sreb2* expression in larger cells that likely reflect spermatogonia (* in Fig. 6D). In contrast, testes in mid-late development exhibited greater divergence among signals located in testicular lobules surrounding the lumen (LU) (Fig. 7). In particular, *sreb3b*-specific expression was detected within testicular lobules in small, dotted patterns within only some cysts, which possibly reflects presence at specific stages of spermatocyte or spermatid growth (dotted circles in Fig. 7A, B, D–F). Larger cells (~10 µm diameter) at the periphery of the testicular lobules but likely inside the basement membrane also exhibited abundant expression of all *sreb* genes (see * in Fig. 7A–C). Smaller cells either at the periphery of testicular lobules or closer to the lumen also exhibited abundant expression (see ** in Fig. 7C, D).

3.5. Absolute quantification of sreb transcripts

Both ovary stages exhibited significantly greater quantities of *sreb1* than any other gene (mean 2562 and 925 mRNA copies/ng total RNA, respectively; $p < 0.001$, Fig. 8). In the primary and early secondary stage ovary, expression of *sreb2* was lower (340 copies/ng RNA) but still significantly greater than either *sreb3a* or *sreb3b* (69 and 121 copies/ng RNA, respectively; $p < 0.01$). However, as transcription decreased in the vitellogenic ovary these three genes all exhibited similar levels. The early developing testis exhibited the overall greatest *sreb* transcription of all gonadal stages and was dominated by similar levels of *sreb1* and *sreb2* expression (5464 and 4958 copies/ng RNA, respectively, Fig. 8). Significantly more *sreb3b* than *sreb3a* was also detected in early testis (826 vs. 274 copies/ng RNA, respectively, $p < 0.05$), but these levels were both less than other genes. Later testicular development was characterized by relative decreases in all genes, but *sreb1* and *sreb2* remained at higher transcript levels (2631 and 1046 copies/ng RNA, respectively) and in most cases, were significantly elevated compared to *sreb3a* (150 copies/ng RNA, $p < 0.01$) and *sreb3b* (381 copies/ng RNA, $p < 0.05$). Overall, gonads were broadly characterized by greater

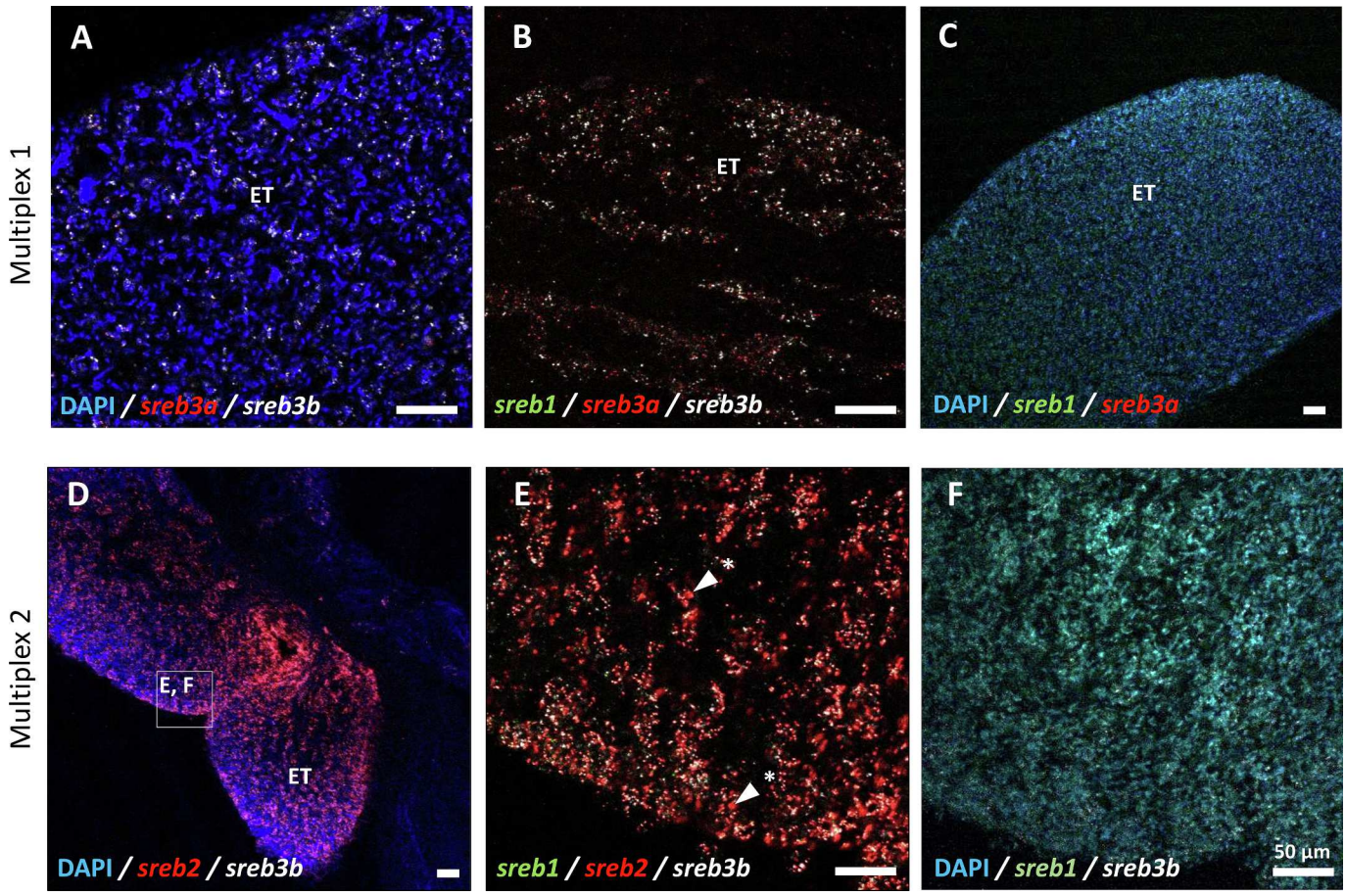

Fig. 6. Multiplex RNAscope of early developing pufferfish testes using Multiplex 1 (*sreb1*, *sreb3a*, and *sreb3b*; A-C) or Multiplex 2 (*sreb*1, *sreb2*, *sreb3b*; D-F). Scale bars refer to 50 µm. Cell nuclei are stained blue using DAPI, and *sreb1* and *sreb3b* are labeled green and white, respectively, while *sreb2* and *sreb3a* are labeled red. The inset square labeled "E, F" in panel D is shown at greater magnification in panels E and F. ET = early testis. * indicates expression in large spermatogonial cells.

expression early in development and were dominated by *sreb1* in ovaries and both *sreb1* and *sreb2* in testes. The *sreb3a* gene consistently exhibited the lowest overall expression in both organs.

4. Discussion

All *sreb* genes exhibited evidence of transcription in both pufferfish ovaries and testes. While this was expected for *sreb2* and *sreb3b*, which are identified as protein-coding genes in the pufferfish genome assembly, this was not assumed for the other two that were annotated as possible pseudogenes (Breton et al., 2021). Such verifications are necessary, as *sreb* loss is not uncommon in some fishes, mammals, and birds (Breton et al., 2021; Stäubert et al., 2022). Results from the present study support pufferfish *sreb1* and *sreb3a* being protein-coding genes, and they are at least not transcriptionally silent. This reinforces past research, where pufferfish genomic DNA sequences confirmed full-length protein-coding regions with no premature stop codons (Breton et al., 2021). As such, the pseudogene annotations for *sreb1* and *sreb3a* instead likely reflect their: 1) characteristics as small, single exons, or 2) reduced gene sizes due to the pufferfish's uniquely compact genome (Crollius et al., 2000). In either case, these genes are actually transcribed and likely both functional and protein-coding, with each *sreb* exhibiting some unique patterns in gonads.

Ovaries exhibited the greatest expression early in oocyte growth, and patterns were largely *sreb1*-dominated. The *sreb1* mRNA was diffuse throughout the ooplasm, which matched patterns for *actb1*, *eef1a*, and *zp3f* that are largely translated before oocyte maturation in vertebrates (Ge et al., 2017; Jansova et al., 2018). Although functions for oocyte *sreb1* are unknown, the receptor regulates glucose metabolism in other cell types (Chopra et al., 2020, Dolanc et al., 2022), and it may play a role in glycolysis before or during fish oocyte maturation (Kang et al., 2021). A similar spatial pattern was observed for the novel *sreb3b*, which could reflect overlapping roles or functions in folliculogenesis and germline pluripotency (Breton et al., 2023). The *sreb3b* gene also exhibited particularly broad expression throughout the early ooplasm, with significantly greater co-localization to all other *sreb* genes, which may indicate diverse functions for this gene in early oocyte growth. Of note, the human paralog *sreb3* is also translated in oocytes (Nguyen et al., 2019), which further reinforces that the diffuse mRNA pattern in ooplasm may indicate a functional role early in ovarian development rather than being a stored transcript.

In contrast, other *sreb* transcripts in oocytes may be stored mRNA, as *sreb2* and *sreb3a* in primary oocytes both exhibited a highly granular appearance. Primary oocytes in vertebrates synthesize large quantities of mRNAs that are not constitutively translated but are instead largely stored for maturation, fertilization, or embryonic development (Wallace and Selman, 1990; Richter, 2007). Examples include *ccnb1* (cyclin B) and *pou5f1* (Oct4), which are synthesized early in the vertebrate oocyte but translated later to act as an oocyte maturation regulator and as an embryonic transcription factor, respectively (Ovitt and Schöler, 1998; Nagahama and Yamashita, 2008; Lubzens et al., 2010). Both of these transcripts exhibit dotted patterns in mammalian oocytes that reflect their storage in RNA granules, and these patterns are both not co-localized and strikingly similar to those observed for *sreb2* and *sreb3a* (see Fig. 4 in Sanada and Kotani, 2024 and compare to Fig. 4 here). Embryonic roles for *sreb2* are not unexpected, as the receptor regulates

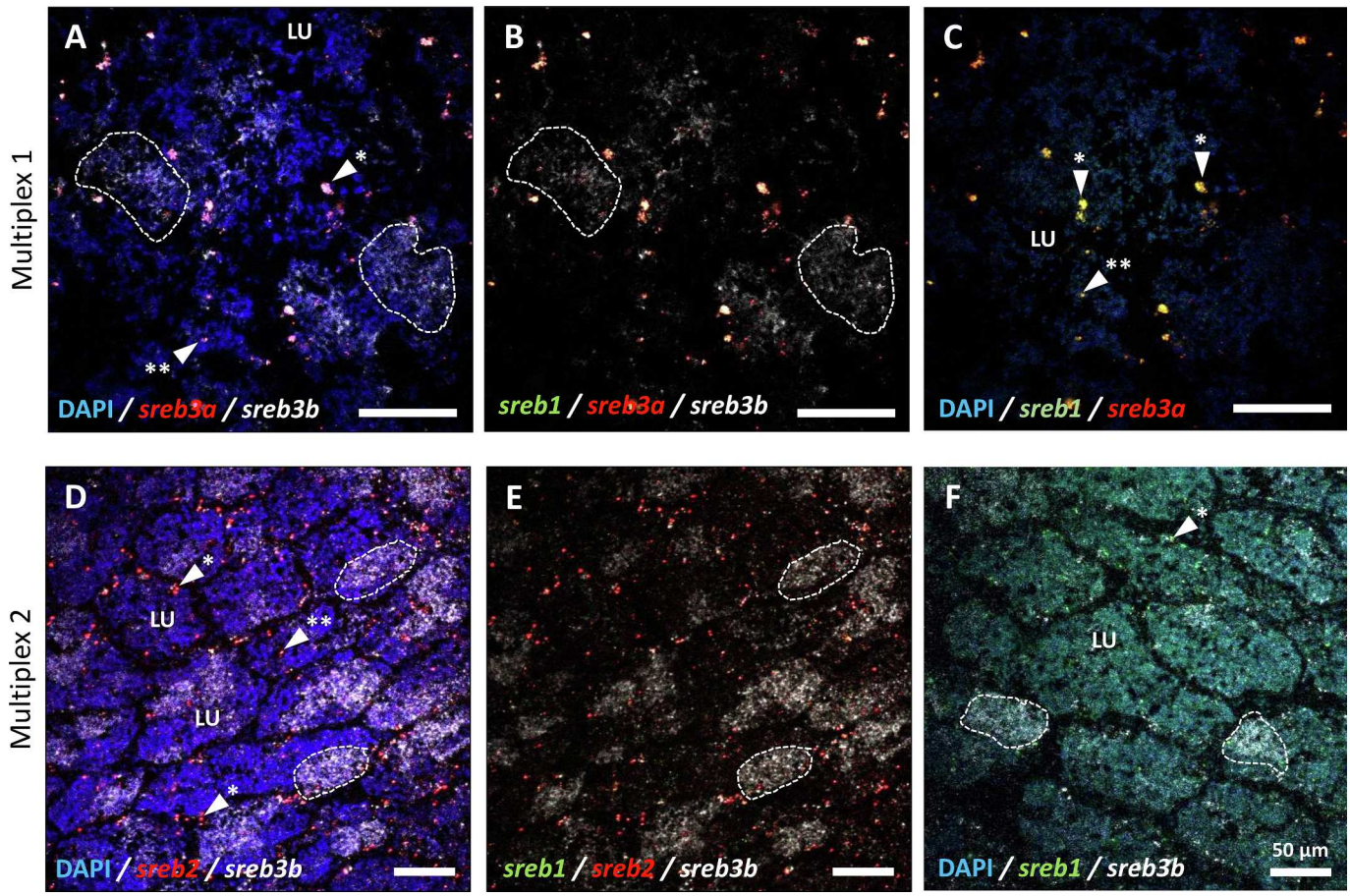

Fig. 7. Multiplex RNAscope of mid to late testicular development in pufferfish using Multiplex 1 (*sreb1*, *sreb3a*, and *sreb3b*; A–C) or Multiplex 2 (*sreb*1, *sreb2*, *sreb3b*; D–F). Scale bars refer to 50 µm. Cell nuclei are stained blue using DAPI, and *sreb1* and *sreb3b* are labeled green and white, respectively, while *sreb2* and *sreb3a* are labeled red. White dotted areas encircle cysts containing *sreb3b*-specific expression. LU = lumen of testicular lobule. * and ** indicate *sreb* expression in likely larger (~10 µm diameter) spermatogonial stem cells and later stage spermatgonia, respectively.

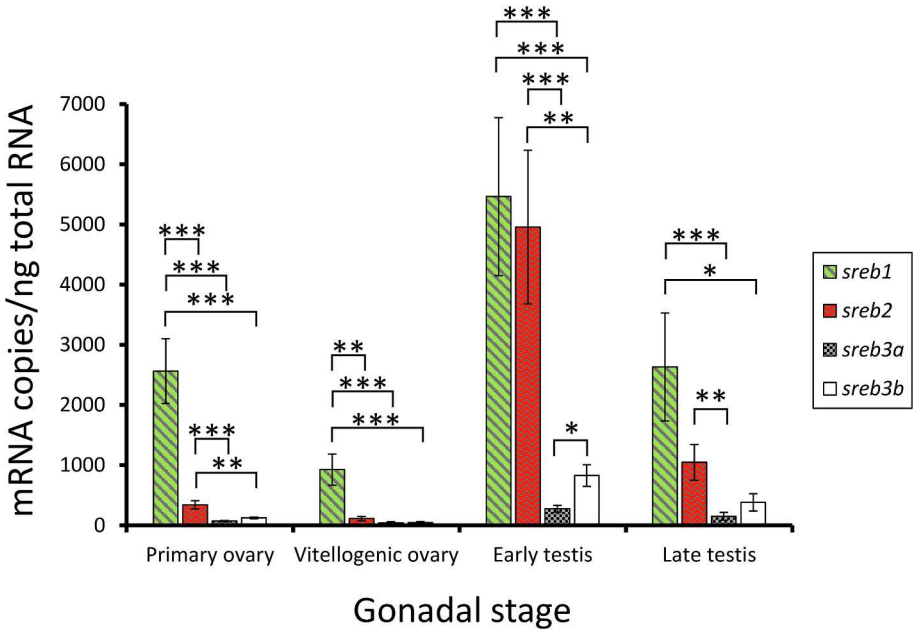

Fig. 8. Absolute qPCR of *sreb* transcripts normalized to input RNA quantity in four pufferfish gonadal stages. Each bar represents the mean ± standard error. Green, red, gray, and white bars refer to *sreb1*, *sreb2*, *sreb3a*, and *sreb3b*, respectively. Significant differences between *sreb* transcripts within a stage are identified in brackets, where *, **, and *** indicate $p < 0.05$, 0.01, and 0.001, respectively.

neuron development in mice and may be associated with organ development and cell proliferation in fish (Matsumoto et al., 2008; Breton et al., 2021, 2023). However, the identification of *sreb2* as a possible maternal mRNA transcript is novel and implicates the receptor in earlier embryonic processes than previously studied. Similarly, *sreb3a* may also have embryonic roles, with related systems functioning in cell growth and neuron migration (Larco et al., 2013; Breton et al., 2022). These roles are still mostly unstudied though, and granule dynamics can be complex (Tauber et al., 2020). For instance, while such germline complexes likely act as reservoirs of translationally repressed but competent mRNAs, they can also function in degradation or be incidental by-products of ongoing cytoplasmic activities that become saturated (Cassani and Seydoux, 2024). Since *sreb3a* is the least expressed of the receptors in pufferfish, these weaker signals may reflect mRNA decay. However, *sreb3a* could also be a low abundance but important stored transcript, as these mRNAs seem to be retained in vitellogenic oocytes.

Ovarian *sreb* patterns were also detected in vitellogenic oocytes, granulosa cells, and small numbers of extra-follicular cells. In vitellogenic oocytes, all *sreb* transcripts were in smaller quantities than during primary growth. Patterns were also restricted to the oocyte periphery and zona pellucida, which is likely the result of accumulating vitellogenins in the central ooplasm and a dramatic decrease in transcriptional activity (De La Fuente and Eppig, 2001; Breton et al., 2022). The control genes also reinforced this and exhibited a similar overall pattern, while identical spatial results were observed for *sreb3b* in killifish (*Nothobranchius furzeri*) (Breton et al., 2021). Just outside the zona pellucida, elevated *sreb* patterns were also detected in granulosa cells of the follicle wall. Granulosa cell SREB3 has previously been found in both human and zebrafish follicles, where the system promotes steroidogenesis and gonadotropin signaling (Nguyen et al., 2019; Rajeswari and Unniappan, 2020). While similar processes are likely present in pufferfish granulosa cells, the presence of all four *sreb* genes implicate overlapping or broader functions for the entire receptor family. Also of note, both prior work and the present study failed to identify robust *sreb* expression in theca cells (Nguyen et al., 2019), meaning that ovarian expression may be greatly reduced outside of granulosa cells. However, small numbers of extra-follicular cells did exhibit expression of *sreb* genes, which may be stromal cells or oogonia undergoing particular metabolic or proliferative processes that need further characterization.

The greatest *sreb* expression was evident in the early testis and likely originated from spermatogonia. Proliferation of spermatogonia is characteristic of prepubertal fish testes, which must generate enough cysts with meiotic spermatocytes to ensure proper testicular development (Schulz et al., 2010). Proliferation begins with undifferentiated spermatogonia that are larger in diameter (~ 10 μm) (Lacerda et al., 2014; Xie et al., 2020). These are the largest germ cells in the fish testis, very low in number, and found near the interstitial regions but inside the basement membrane (Schulz et al., 2010; Xie et al., 2020). Cells with these characteristics were identified in the pufferfish testes and exhibited elevated *sreb* expression. Prior research also identified that early pufferfish testes exhibit the greatest expression across gonadal stages (Breton et al. 2021), which was reinforced in the present study. The current work, however, also highlights that both *sreb1* and *sreb2* are expressed at significantly greater levels in these cells than the other receptor genes. Expression was also clear in smaller cells inside lobules in mid-late testes, which probably reflects differentiating spermatogonia as they decrease in size (Lacerda et al., 2014). Elevated expression in these cells may function in stem cell maintenance, as many GPCRs, including all three mammalian *sreb* members, are upregulated in pluripotent stem cells and regulate self-renewal (Choi et al., 2015). Such roles are also supported by the relative dominance in testicular tissues of both *sreb1* and *sreb2*, which likely regulate proliferation (Matsumoto et al., 2008; Wang et al., 2022; Breton et al., 2023).

Lastly, while all *sreb* genes were detected in testicular mitotic cells, their expression was restricted in meiotic cells. Only *sreb3b* was identified in some spermatogenic cysts in the mid-late testes, but expression was likely limited to either spermatocyte or spermatid developmental stages. Similar patterns for zebrafish SREB3A were previously found, but specific staging also was unclear (Rajeswari and Unniappan, 2020). Overall, there is very little information on *sreb* expression in meiotic cells in any vertebrate testis. However, specific patterns observed in pufferfish indicate that the fish-specific *sreb3b* likely exhibits novel roles that are distinct from the other receptors. As such, future research is warranted to better understand *sreb3b* functions in both oocytes and spermatogenic cells, which could provide new insights into the regulation of gamete development in fish.

5. Conclusion

The *sreb* receptor family is expressed in both pufferfish ovaries and testes, and patterns reflect possible roles in oocyte growth, embryonic development, and spermatogonial cell proliferation. In particular, *sreb1* and *sreb2* exhibited the greatest overall expression in all stages. Expression patterns for *sreb3b* were unique in both oocytes and spermatogenic cells, which may indicate novel gamete-specific reproductive roles. Lastly, both *sreb3a* and *sreb2* may be stored mRNA transcripts in oocytes. These complex spatial patterns highlight how little is known about these receptors in any vertebrate, and future studies will be critical to unravel SREB roles in both ovarian and testicular development.

CRediT authorship contribution statement

Timothy S. Breton: Writing – review & editing, Writing – original draft, Visualization, Validation, Supervision, Resources, Project administration, Methodology, Investigation, Funding acquisition, Formal analysis, Conceptualization. **Maria Eduarda Oliveira:** Writing – review & editing, Supervision, Investigation, Formal analysis. **Truly Chillemi:** Writing – review & editing, Supervision, Investigation, Formal analysis. **William Harriman:** Writing – review & editing, Investigation, Formal analysis. **Joanna Korasadowicz:** Writing – review & editing, Investigation, Formal analysis. **Eme Saverese:** Writing – review & editing, Supervision, Investigation, Formal analysis. **Emma Bourget:** Writing – review & editing, Investigation, Formal analysis. **Casey A. Murray:** Writing – review & editing, Project administration, Investigation, Funding acquisition, Conceptualization. **Christopher J. Martyniuk:** Writing – review & editing, Project administration, Funding acquisition, Conceptualization. **Matthew A. DiMaggio:** Writing – review & editing, Project administration, Funding acquisition, Conceptualization.

Declaration of Competing Interest

The authors declare that they have no known competing financial interests or personal relationships that could have appeared to influence the work reported in this paper.

Acknowledgements

This material is based upon work supported by the National Science Foundation under Award No. 2307614. Research reported in this project was supported by an Institutional Development Award (IDeA) from the National Institute of General Medical Sciences (NIGMS) of the National Institutes of Health (NIH) under grant number P20GM103423. T.S.B. was supported by the University of Maine at Farmington (UMF) under the 2023-2024 Trustee Professorship. M.E.O. and T.C. were supported through 2024 Maine-INBRE Summer Undergraduate Research Fellowships. We thank Jean Doty and Hannah Lust from UMF and MDI Biological Laboratory, respectively, for the student fellowship opportunities. We thank Dustin Updike and Frederic Bonnet from MDI Biological Laboratory for providing the confocal microscope used in this study. Image collection was performed with the assistance of the MDI Biological Laboratory Light Microscopy Facility (RRID:SCR_019166), which is also supported by NIH NIGMS grant number P20GM103423.

We thank Erin Osborne Nishimura from Colorado State University for helpful insight on P-body-like granules. We thank Natasha Goldman from WISSEN, Inc. and James Pann for project proposal assistance. We thank Noah Young and Noelle Dubay from the UMF TRIO Upward Bound Program for project assistance. Lastly, we thank Jordan Leavitt and Angela Carter from UMF for project support.

Appendix A. Supplementary data

Supplementary data to this article can be found online at https://doi.org/10.1016/j.ygcen.2024.114641.

Data availability

Data will be made available on request.

References

Breton, T.S., Kenter, L.W., Greenlaw, K., Montgomery, J., Goetz, G.W., Berlinsky, D.L., Luckenbach, J.A., 2019. Initiation of sex change and gonadal gene expression in black sea bass (*Centropristis striata*) exposed to exemestane, an aromatase inhibitor. Comp. Biochem. Physiol. Part A Mol. Integr. Physiol. 228, 51–61. https://doi.org/10.1016/j.cbpa.2018.10.024.

Breton, T.S., Sampson, W.G., Clifford, B., Phaneuf, A.M., Smidt, I., True, T., Wilcox, A.R., Lipscomb, T., Murray, C., DiMaggio, M.A., 2021. Characterization of the G protein-coupled receptor family SREB across fish evolution. Sci. Rep. 11, 12066. https://doi.org/10.1038/s41598-021-91590-9.

Breton, T.S., Murray, C.A., Huff, S.R., Phaneuf, A.M., Tripp, B.M., Patuel, S.J., Martyniuk, C.J., DiMaggio, M.A., 2022. Phoenixin-14 alters transcriptome and steroid profiles in female green-spotted puffer (*Dichotomyctere nigroviridis*). Sci. Rep. 12, 9454. https://doi.org/10.1038/s41598-022-13695-z.

Breton, T.S., Fike, S., Francis, M., Patnaude, M., Murray, C.A., DiMaggio, M.A., 2023. Characterizing the SREB G protein-coupled receptor family in fish: Brain gene expression and genomic differences in upstream transcription factor binding sites. Comp. Biochem. Physiol. Part A Mol. Integr. Physiol. 285, 111507. https://doi.org/10.1016/j.cbpa.2023.111507.

Campbell, B., Dickey, J., Beckman, B., Young, G., Pierce, A., Fukada, H., Swanson, P., 2006. Previtellogenic oocyte growth in salmon: relationships among body growth, plasma insulin-like growth factor-1, estradiol-17beta, follicle-stimulating hormone and expression of ovarian genes for insulin-like growth factors, steroidogenic-acute regulatory protein and receptors for gonadotropins, growth hormone, and somatolactin. Biol. Reprod. 75, 34–44. https://doi.org/10.1095/biolreprod.105.049494.

Cassani, M., Seydoux, G., 2024. P-body-like condensates in the germline. Sem. Cell Dev. Biol. 157, 24–32. https://doi.org/10.1016/j.semcdb.2023.06.010.

Chen, Q., Kogan, J.H., Gross, A.K., Zhou, Y., Walton, N.M., Shin, R., Heusner, C.L., Miyake, S., Tajinda, K., Tamura, K., Matsumoto, M., 2012. SREB2/GPR85, a schizophrenia risk factor, negatively regulates hippocampal adult neurogenesis and neurogenesis dependent learning and memory. Eur. J. Neurosci. 36, 2597–2608. https://doi.org/10.1111/j.1460-9568.2012.08180.x.

Choi, H.Y., Saha, S.K., Kim, K., Kim, S., Yang, G.M., Kim, B., Kim, J.H., Cho, S.G., 2015. G protein-coupled receptors in stem cell maintenance and somatic reprogramming to pluripotent or cancer stem cells. Bmbrep. 48, 68–80. https://doi.org/10.5483/BMBRep.2015.48.2.250.

Chopra, D.G., Yiv, N., Hennings, T.G., Zhang, Y., Ku, G.M., 2020. Deletion of Gpr27 in vivo reduces insulin mRNA but does not result in diabetes. Sci. Rep. 10, 5629. https://doi.org/10.1038/s41598-020-62358-4.

Conte, J., Potoczniak, M.J., Tobe, S.S., 2018. Using synthetic oligonucleotides as standards in probe-based qPCR. BioTechniques 64, 177–179. https://doi.org/10.2144/btn-2018-2000.

Crollius, H.R., Jaillon, O., Dasilva, C., Ozouf-Costaz, C., Fizames, C., Fischer, C., Bouneau, L., Billault, A., Quetier, F., Saurin, W., Bernot, A., 2000. Characterization and repeat analysis of the compact genome of the freshwater pufferfish *Tetraodon nigroviridis*. Genome Res. 10, 939–949. https://doi.org/10.1101/gr.10.7.939.

De La Fuente, R., Eppig, J.J., 2001. Transcriptional activity of the mouse oocyte genome: Companion granulosa cells modulate transcription and chromatin remodeling. Dev. Biol. 229, 224–236. https://doi.org/10.1006/dbio.2000.9947.

Dolanc, D., Zorec, T.M., Smole, Z., Maver, A., Horvat, A., Pillaiyar, T., Trkov Bobnar, S., Vardjan, N., Kreft, M., Chowdhury, H.H., Zorec, R., 2022. The activation of GPR27 increases cytosolic L-lactate in 3T3 embryonic cells and astrocytes. Cells 11, 1009. https://doi.org/10.3390/cells11061009.

Fujita-Jimbo, E., Tanabe, Y., Yu, Z., Kojima, K., Mori, M., Li, H., Iwamoto, S., Yamagata, T., Momoi, M.Y., Momoi, T., 2015. The association of GPR85 with PSD-95-neuroligin complex and autism spectrum disorder: a molecular analysis. Mol. Autism 6, 17. https://doi.org/10.1186/s13229-015-0012-5.

Ge, C., Lu, W., Chen, A., 2017. Quantitative proteomic reveals the dynamic of protein profile during final oocyte maturation in zebrafish. Biochem. Biophys. Res. Comm. 490, 657–663. https://doi.org/10.1016/j.bbrc.2017.06.093.

He, L., Shi, H., Zhang, G., Peng, Y., Ghosh, A., Zhang, M., Hu, X., Liu, C., Shao, Y., Wang, S., Chen, L., 2023. A novel CCK receptor GPR173 mediates potentiation of GABAergic inhibition. J. Neurosci. 43, 2305–2325. https://doi.org/10.1523/JNEUROSCI.2035-22.2023.

Hellebrand, S., Schaller, H.C., Wittenberger, T., 2000. The brain-specific G-protein coupled receptor GPR85 with identical protein sequence in man and mouse maps to human chromosome 7q31. Biochim. Biophys. Acta 1493, 269–272. https://doi.org/10.1016/S0167-4781(00)00182-2.

Jansova, D., Tetkova, A., Koncicka, M., Kubelka, M., Susor, A., 2018. Localization of RNA and translation in the mammalian oocyte and embryo. e0192544 PLoS ONE 13. https://doi.org/10.1371/journal.pone.0192544.

Jiang, M., Liu, J., Jiang, D., Pan, Q., Shi, H., Huang, Y., Zhu, C., Li, G., Deng, S., 2022. Characterization and expression analysis of *gpr173a* and *gpr173b* revealed their involvement in reproductive regulation in spotted scat (*Scatophagus argus*), 101239 Aquacult. Rep. 25. https://doi.org/10.1016/j.aqrep.2022.101239.

Kalamon, N., Błaszczyk, K., Szlaga, A., Billert, M., Skrzypski, M., Pawlicki, P., Górowska-Wójtowicz, E., Kotula-Balak, M., Błasiak, A., Rak, A., 2020. Levels of the neuropeptide phoenixin-14 and its receptor GRP173 in the hypothalamus, ovary and periovarian adipose tissue in rat model of polycystic ovary syndrome. Biochem. Biophys. Res. Commun. 528, 628–635. https://doi.org/10.1016/j.bbrc.2020.05.101.

Kang, T., Zhao, S., Shi, L., Li, J., 2021. Glucose metabolism is required for oocyte maturation of zebrafish. Biochem. Biophys. Res. Comm. 559, 191–196. https://doi.org/10.1016/j.bbrc.2021.04.059.

Ku, G.M., Pappalardo, Z., Luo, C.C., German, M.S., McManus, M.T., 2012. An siRNA screen in pancreatic beta cells reveals a role for gpr27 in insulin production. e1002449 PLoS Genetics 8. https://doi.org/10.1371/journal.pgen.1002449.

Lacerda, S.M.D.S.N., Costa, G.M.J., de França, L.R., 2014. Biology and identity of fish spermatogonial stem cell. Gen. Comp. Endocrinol. 207, 56–65. https://doi.org/10.1016/j.ygcen.2014.06.018.

Larco, D.O., Semsarzadeh, N.N., Cho-Clark, M., Mani, S.K., Wu, T.J., 2013. The novel actions of the metabolite GnRH-(1–5) are mediated by a G protein-coupled receptor. Front. Endocrinol. 4, 83. https://doi.org/10.3389/fendo.2013.00083.

Larco, D.O., Bauman, B.M., Cho-Clark, M., Mani, S.K., Wu, T.J., 2018. GnRH-(1–5) inhibits TGF-β signaling to regulate the migration of immortalized gonadotropin-releasing hormone neurons. Front. Endocrinol. 9, 45. https://doi.org/10.3389/fendo.2018.00045.

Lubzens, E., Young, G., Bobe, J., Cerdà, J., 2010. Oogenesis in teleosts: how fish eggs are formed. Gen. Comp. Endocrinol. 165, 367–389. https://doi.org/10.1016/j.ygcen.2009.05.022.

Mascalchi, P., Cordelières, F.P., 2019. Which elements to build co-localization workflows? From metrology to analysis. In: Rebollo, E., Bosch, M. (eds) Computer Optimized Microscopy. Methods in Molecular Biology, vol 2040. Humana, New York, NY.

Matsumoto, M., Saito, T., Takasaki, J., Kamohara, M., Sugimoto, T., Kobayashi, M., Tadokoro, M., Matsumoto, S.I., Ohishi, T., Furuichi, K., 2000. An evolutionarily conserved G-protein coupled receptor family, SREB, expressed in the central nervous system. Biochem. Biophys. Res. Commun. 272, 576–582. https://doi.org/10.1006/bbrc.2000.2829.

Matsumoto, M., Beltaifa, S., Weickert, C.S., Herman, M.M., Hyde, T.M., Saunders, R.C., Lipska, B.K., Weinberger, D.R., Kleinman, J.E., 2005. A conserved mRNA expression profile of SREB2 (GPR85) in adult monkey, human, and rat forebrain. Mol. Brain Res. 138, 58–69. https://doi.org/10.1016/j.molbrainres.2005.04.002.

Matsumoto, M., Straub, R.E., Marenco, S., Nicodemus, K.K., Matsumoto, S.I., Fujikawa, A., Miyoshi, S., Shobo, M., Takahashi, S., Yarimizu, J., Yuri, M., 2008. The evolutionarily conserved G protein-coupled receptor SREB2/GPR85 influences brain size, behavior, and vulnerability to schizophrenia. Proc. Natl. Acad. Sci. 105, 6133–6138. https://doi.org/10.1073/pnas.0710717105.

McIlwraith, E.K., Belsham, D.D., 2018. Phoenixin: uncovering its receptor, signaling and functions. Acta Pharmacol. Sin. 39, 774–778. https://doi.org/10.1038/aps.2018.13.

McIlwraith, E.K., Zhang, N., Belsham, D.D., 2022. The regulation of phoenixin: a fascinating multidimensional peptide. bvab192 J. Endo. Soc. 6. https://doi.org/10.1210/jendso/bvab192.

Nagahama, Y., Yamashita, M., 2008. Regulation of oocyte maturation in fish. Dev. Growth Differ. 50, S195–S219. https://doi.org/10.1111/j.1440-169X.2008.01019.x.

Nguyen, X.P., Nakamura, T., Osuka, S., Bayasula, B., Nakanishi, N., Kasahara, Y., Muraoka, A., Hayashi, S., Nagai, T., Murase, T., Goto, M., 2019. Effect of the neuropeptide phoenixin and its receptor GPR173 during folliculogenesis. Reproduction 158, 24–34. https://doi.org/10.1530/REP-19-0025.

O'Dowd, B.F., Nguyen, T., Marchese, A., Cheng, R., Lynch, K.R., Heng, H.H., Kolakowski Jr, L.F., George, S.R., 1998. Discovery of three novel G-protein-coupled receptor genes. Genomics 47, 310–313. https://doi.org/10.1006/geno.1998.5095.

Ovitt, C.E., Schöler, H.R., 1998. The molecular biology of Oct-4 in the early mouse embryo. Mol. Human Reprod. 4, 1021–1031. https://doi.org/10.1093/molehr/4.11.1021.

Picha, M.E., Turano, M.J., Tipsmark, C.K., Borski, R.J., 2008. Regulation of endocrine and paracrine sources of Igfs and Gh receptor during compensatory growth in hybrid striped bass (*Morone chrysops* × *Morone saxatilis*). J. Endocrinol. 199, 81–94. https://doi.org/10.1677/JOE-07-0649.

Rajeswari, J.J., Unniappan, S., 2020. Phoenixin-20 stimulates mRNAs encoding hypothalamo-pituitary-gonadal-hormones, is provitellogenic, and promotes oocyte maturation in zebrafish. Sci. Rep. 10, 6264. https://doi.org/10.1038/s41598-020-63226-x.

Regard, J.B., Kataoka, H., Cano, D.A., Camerer, E., Yin, L., Zheng, Y.W., Scanlan, T.S., Hebrok, M., Coughlin, S.R., 2007. Probing cell type-specific functions of Gi in vivo identifies GPCR regulators of insulin secretion. J. Clin. Invest. 117, 4034–4043. https://doi.org/10.1172/JCI32994.

Richter, J.D., 2007. CPEB: a life in translation. Trends Biochem. Sci. 32, 279–285. https://doi.org/10.1016/j.tibs.2007.04.004.

Rybska, M., Billert, M., Skrzypski, M., Kubiak, M., Woźna-Wysocka, M., Łukomska, A., Nowak, T., Błaszczyk-Cichoszewska, J., Pomorska-Mól, M., Wąsowska, B., 2022. Canine cystic endometrial hyperplasia and pyometra may downregulate neuropeptide phoenixin and GPR173 receptor expression. Anim. Reprod. Sci. 238, 106931. https://doi.org/10.1016/j.anireprosci.2022.106931.

Rybska, M., Billert, M., Skrzypski, M., Wojciechowicz, T., Kubiak, M., Łukomska, A., Nowak, T., Włodarek, J., Wąsowska, B., 2023. Expression and localization of the neuropeptide phoenixin-14 and its receptor GRP173 in the canine reproductive organs and periovarian adipose tissue. Anim. Reprod. Sci. 255, 107282. https://doi.org/10.1016/j.anireprosci.2023.107282.

Sanada, T., Kotani, T., 2024. High-sensitivity whole-mount in situ Hybridization of Mouse Oocytes and Embryos Visualizes the Super-resolution Structures and Distributions of mRNA Molecules. Biol. Proced. Online 26, 23. https://doi.org/10.1186/s12575-024-00250-5.

Schindelin, J., Arganda-Carreras, I., Frise, E., Kaynig, V., Longair, M., Pietzsch, T., Preibisch, S., Rueden, C., Saalfeld, S., Schmid, B., Tinevez, J.Y., 2012. Fiji: an open-source platform for biological-image analysis. Nat. Methods 9, 676–682. https://doi.org/10.1038/nmeth.2019.

Schriewer, A., Wehlmann, A., Wuertz, S., 2011. Improving qPCR efficiency in environmental samples by selective removal of humic acids with DAX-8. J. Microbiol. Methods 85, 16–21. https://doi.org/10.1016/j.mimet.2010.12.027.

Schulz, R.W., de França, L.R., Lareyre, J.J., LeGac, F., Chiarini-Garcia, H., Nobrega, R.H., Miura, T., 2010. Spermatogenesis in fish. Gen. Comp. Endocrinol. 165, 390–411. https://doi.org/10.1016/j.ygcen.2009.02.013.

Stäubert, C., Wozniak, M., Dupuis, N., Laschet, C., Pillaiyar, T., Hanson, J., 2022. Superconserved receptors expressed in the brain: Expression, function, motifs and evolution of an orphan receptor family. Pharmacol. Ther. 240, 108217. https://doi.org/10.1016/j.pharmthera.2022.108217.

Tauber, D., Tauber, G., Parker, R., 2020. Mechanisms and regulation of RNA condensation in RNP granule formation. Trends Biochem. Sci. 45, P764–P778. https://doi.org/10.1016/j.tibs.2020.05.002.

Wallace, R.A., Selman, K., 1990. Ultrastructural aspects of oogenesis and oocyte growth in fish and amphibians. J. Electron Microsc. Tech. 16, 175–201. https://doi.org/10.1002/jemt.1060160302.

Wang, H., Du, D., Huang, J., Wang, S., He, X., Yuan, S., Xiao, J., 2022. GPR27 regulates hepatocellular carcinoma progression via MAPK/ERK pathway. Cancer Manag. Res. 14, 1165–1177. https://doi.org/10.2147/CMAR.S335749.

Wang, F., Flanagan, J., Su, N., Wang, L.C., Bui, S., Nielson, A., Wu, X., Vo, H.T., Ma, X.J., Luo, Y., 2012. RNAscope: a novel in situ RNA analysis platform for formalin-fixed, paraffin-embedded tissues. J. Mol. Diagnostics 14, 22–29. https://doi.org/10.1016/j.jmoldx.2011.08.002.

Xie, X., Nóbrega, R., Pšenička, M., 2020. Spermatogonial stem cells in fish: characterization, isolation, enrichment, and recent advances of in vitro culture systems. Biomol. 10, 644. https://doi.org/10.3390/biom10040644.

Yosten, G.L., Lyu, R.M., Hsueh, A.J., Avsian-Kretchmer, O., Chang, J.K., Tullock, C.W., Dun, S.L., Dun, N., Samson, W.K., 2013. A novel reproductive peptide, phoenixin. J. Neuroendocrinol. 25, 206–215. https://doi.org/10.1111/j.1365-2826.2012.02381.x.